PROCEEDINGS OF SCIENCE

Parity violating single spin asymmetry in W production from longitudinally polarized p+p collisions at 500 GeV

John S. Haggerty[*†]
Brookhaven National Laboratory
E-mail: haggerty@bnl.gov

Large parity violating longitudinal single-spin asymmetries $A_L^{e^+} = -0.86^{+0.30}_{-0.14}$ and $A_L^{e^-} = 0.88^{+0.12}_{-0.71}$ are observed for inclusive high transverse momentum electrons and positrons in polarized $p+p$ collisions at a center of mass energy of $\sqrt{s} = 500\,\text{GeV}$ with the PHENIX detector at RHIC. These $e^{\pm}$ come mainly from the decay of $W^{\pm}$ and Z^0 bosons, and their asymmetries directly demonstrate parity violation in the couplings of the $W^{\pm}$ to the light quarks. The observed electron and positron yields were used to estimate $W^{\pm}$ boson production cross sections for the $e^{\pm}$ decays of the $W^{\pm}$.

35th International Conference of High Energy Physics
July 22-28, 2010
Paris, France

[*]Speaker.
[†]Representing the PHENIX collaboration.

PoS(ICHEP 2010)149

The cross sections and longitudinal single spin asymmetries from $pp \to e^{\pm}X$ in polarized pp collisions at $\sqrt{s} = 500$ GeV have been measured with the PHENIX and STAR detectors at RHIC [1, 2]. Events were collected during the initial operation of RHIC at a center of mass energy of 500 GeV in 2009 by selecting events with large energy deposits in electromagnetic calorimeters which predominantly come from decays of W and Z bosons to electrons and positrons.

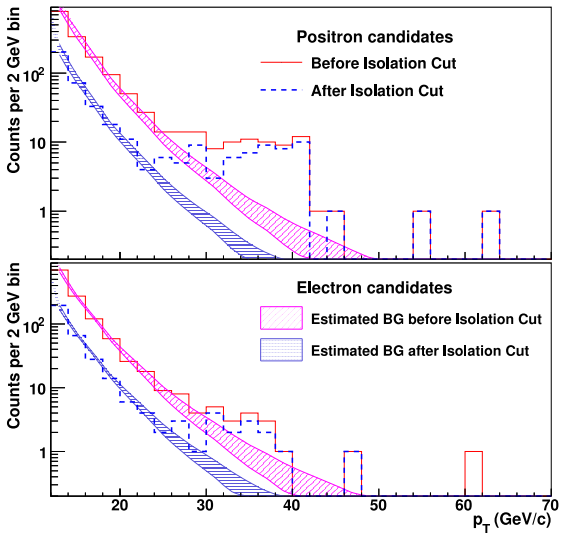

Figure 1: The spectra of positron (upper panel) and electron (lower panel) candidates before (solid histogram) and after (dashed histogram) an isolation cut. The estimated background bands are also shown.

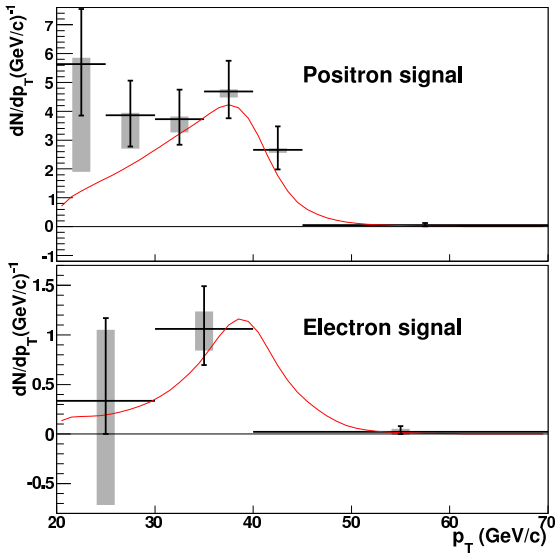

Figure 2: Background subtracted spectra of positron (upper panel) and electron (lower panel) candidates before the isolation cut compared to the spectrum of W and Z decays from an NLO calculation. The gray bands reflect the maximum extent of background estimates.

1. Detector and Analysis

The PHENIX detector has been described in detail elsewhere [8]. This analysis is based on data collected with two central arm spectrometers, each covering $|\Delta\phi| < \pi/2$ in azimuth and $|\eta| < 0.35$ in pseudorapidity, which surround the central axial magnetic field. The bend angle of charged tracks is determined by tracking chambers outside the magnetic field starting at a radius of 2 m from the beamline. An electromagnetic calorimeter, located at a radial distance of 5 m from the beam line, is used to measure the energy, position, and time of flight of electrons. The p_T dependence of π^0 and η widths was used to determine the energy resolution $\sigma_E/E = 8.1\%/\sqrt{E(GeV)} \bigoplus 5.0\%$.

An electromagnetic trigger fully efficient for $e^{\pm}$ with p_T above 12 GeV/c was used to select events for this analysis. Events with a longitudinal vertex position well within the acceptance of the central arm spectrometers were analyzed, and loose cuts on the time of flight measured by the calorimeter and energy-momentum matching suppressed accidental matches and cosmic rays. The analyzed data sample corresponds to an integrated luminosity of 8.6 pb^{-1}, which was corrected for a small (6%) effect of multiple collisions per beam crossing.

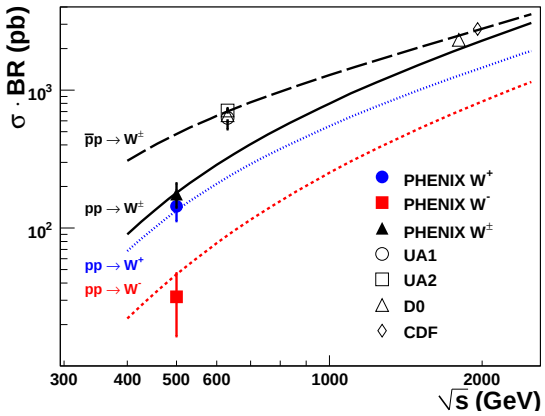

Figure 3: Inclusive cross sections for W leptonic decay channel of this measurement and $\bar{p}p$ measurements [3–6]. Statistical and systematic uncertainties were added here in quadrature. Curves represent theory calculations.

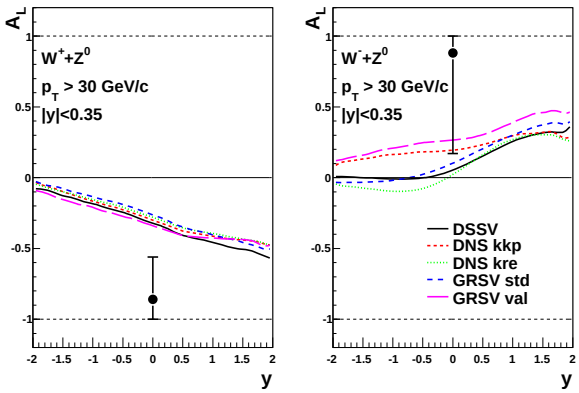

Figure 4: Longitudinal single-spin asymmetries for electrons and positrons from W and Z decays. The error bars represent 68% CL. The theoretical curves are calculated using NLO with different polarized PDFs [7].

The spectrum of electron and positron candidates is shown in Fig. 1 where p_T has been determined from the calorimeter cluster energy and position. The charge sign is determined from the bend angle of the track in the drift chamber, which is about 2.3 mr for a track with momentum of 40 GeV/c with a resolution typically about 1.1 mr. The resulting charge misidentification at 40 GeV/c was estimated to be less than 2%.

In addition to $e^{\pm}$ from W and Z decay, this sample of events contains various backgrounds. The dominant backgrounds were photon conversions before the drift chamber and charged hadrons which were estimated by a combination of simulation and data. The background bands in Fig. 1 include uncertainties in the photon conversion probability, the background normalization, and the background extrapolation to $p_T > 30$ GeV/c.

The tracks within the nominal geometric acceptance of the central spectrometer were reconstructed with $\sim 37\%$ efficiency defined by the overlap of live areas in the tracking detectors, and fiducial cuts on the calorimeters and drift chambers. The efficiency for retaining electron candidates after all cuts was 99%.

Figure 2 shows the background subtracted signal in the acceptance of the detector for positive and negative charges. They are compared to the spectrum predicted by NLO calculations [7, 9, 10] normalized for the integrated luminosity, corrected for the detector efficiency and acceptance, and smeared by the energy resolution of the calorimeter. The yield measured by counting events in the signal ($30 < p_T < 50$ GeV/c) region is compared to the predicted yield in Table 1.

2. $W^{\pm}$ Cross Section

To compute the $W^{\pm}$ production cross section, we subtracted the estimated Z contribution in our sample and the unobserved part of the spectrum with the NLO and NNLO (FEWZ[10]) calculations and MRST [11] and MSTW [12] PDFs according to $\Delta\eta \frac{d\sigma}{d\eta} f_W^{\pm}/s^{\pm}$ where $f_W^{\pm}$ is the fraction of the

Table 1: Comparison of measured cross sections for electrons and positrons with $30 < p_T < 50$ GeV/c from W and Z decays with NLO [7] and NNLO [10] calculations. The first error is statistical, the second error is systematic from the uncertainty in the background, the third error is a normalization uncertainty.

	$\frac{d\sigma}{dy}(30 < p_T^e < 50\,\mathrm{GeV}/c)\|_{y=0}$ [pb]		
Lepton	Data	NLO	NNLO
e^+	$50.2 \pm 7.2^{+1.2}_{-3.6} \pm 7.5$	43.2	46.8
e^-	$9.7 \pm 3.7^{+2.1}_{-2.5} \pm 1.5$	11.3	13.5
e^+ and e^-	$59.9 \pm 8.1^{+3.1}_{-6.0} \pm 9.0$	54.5	60.3

spectrum from W decay (0.9308 for e^+ and 0.6936 for e^-) and $s^{\pm}$ is the observed fraction of the W spectrum (0.2269 for W^+ and 0.1487 for W^-). With these corrections, $\sigma(pp \to W^+X) \times BR(W^+ \to e^+\nu_e) = 144.1 \pm 21.2(\mathrm{stat})^{+3.4}_{-10.3}(\mathrm{syst}) \pm 15\%(norm)$ pb, and $\sigma(pp \to W^-X) \times BR(W^- \to e^-\bar{\nu_e}) = 31.7 \pm 12.1(\mathrm{stat})^{+10.1}_{-8.2}(\mathrm{syst}) \pm 15\%(norm)$ pb, where BR is the branching ratio. These are shown in Fig. 3 and compared to published Tevatron and S$p\bar{p}$S data [3–6]. The systematic uncertainties in the measurement include the uncertainty in the background and a 15% normalization uncertainty due to the luminosity (10%), multiple collision (5%), and acceptance and efficiency uncertainties (10%).

3. Longitudinal Spin Asymmetry

In order to determine the longitudinal spin asymmetry with a sample of W decays with minimal background contamination, two additional requirements were imposed on the candidate events. Events with tracks which had a bend angle < 1 mr were rejected, which reduces charge misidentification to negligible levels, and an isolation cut, requiring the sum of cluster energies in the calorimeter and transverse momenta measured in the drift chamber be less than 2 GeV in a cone with a radius in η and ϕ of 0.5 around the candidate track, was used to remove remaining events with jets. There are 42 candidate $W^+ + Z^0$ decays to positrons with a background of 1.7 ± 1.0 and 13 candidate $W^- + Z^0$ decays to electrons with a background of 1.6 ± 1.0 events within $30 < p_T < 50$ GeV/c after these two additional cuts.

The longitudinal spin asymmetry is determined from the measured asymmetry, ε_L, by

$$\varepsilon_L = \frac{N^+ - R \cdot N^-}{N^+ + R \cdot N^-} \quad A_L = \frac{\varepsilon_L \cdot D}{P} \tag{3.1}$$

where N^+ is the number of events from a beam of positive helicity, N^- is the number of events from a beam of negative helicity, R is the relative luminosity of positive and the negative helicity beams, P is the beam polarization, and D is a dilution correction to account for the remaining background in the signal region. The two RHIC beams, with luminosity-weighted average polarizations of 0.38 ± 0.03 and 0.40 ± 0.04, provide independent measurements of A_L. Both beams are bunched, and the bunch helicity alternates almost every crossing to reduce systematic effects. A likelihood function created from the four spin sorted yields corresponding to the two polarized beams was used to determine the single-spin asymmetry within its physical range [−1,1].

The measured asymmetries are shown in Table 2 for tracks in the background ($12 < p_T < 20$ GeV/c) and signal ($30 < p_T < 50$ GeV/c) regions. For tracks in the background region, ε_L was

Table 2: Longitudinal single-spin asymmetries. The confidence intervals are defined for A_L^e.

Sample	ε_L	$A_L^e(W+Z)$	68% CL	95% CL
Positive background	-0.015 ± 0.04			
Positive signal	-0.31 ± 0.10	-0.86	$[-1,-0.56]$	$[-1,-0.16]$
Negative background	-0.025 ± 0.04			
Negative signal	0.29 ± 0.20	$+0.88$	$[0.17,1]$	$[-0.60,1]$

found to be zero within uncertainties. A significant non-zero asymmetry was observed for positrons in the signal region.

Figure 4 compares measured longitudinal single-spin asymmetries to estimates based on a sample of polarized PDFs extracted from fits of DIS and semi-inclusive DIS data [7]. The experimental results are consistent with the theoretical calculations at 6-15% confidence level for $A_L^{e^+}$ and at 20-37% for $A_L^{e^-}$. The observed asymmetries are sensitive to the polarized quark densities at $x \sim M_W/\sqrt{s} \simeq 0.16$, and directly demonstrate the parity violating coupling between W bosons and light quarks.

4. Summary

In summary, we presented first measurements of production cross section and nonzero parity violating asymmetry in W and Z production in polarized $p+p$ collisions at $\sqrt{s} = 500$ GeV. The results are found to be consistent with theoretical expectations and similar measurements of $A_L^{e^\pm}$ [2]. RHIC luminosity and PHENIX detector upgrades in progress will make it possible in the future to significantly reduce the uncertainties for A_L and to extend the measurement to forward rapidity, which will improve our knowledge of flavor separated quark and antiquark helicity distributions.

References

[1] A. Adare *et al.* arXiv:1009:0505, to be published.

[2] M. M. Aggarwal *et al.* arXiv:1009.0326, to be published.

[3] D. E. Acosta *et al. Phys. Rev. Lett.* **94** (2005) 091803.

[4] B. Abbott *et al. Phys. Rev.* **D61** (2000) 072001.

[5] J. Alitti *et al. Z. Phys.* **C47** (1990) 11–22.

[6] C. Albajar *et al. Z. Phys.* **C44** (1989) 15–61.

[7] D. de Florian and W. Vogelsang *Phys. Rev.* **D81** (2010) 094020.

[8] K. Adcox *et al. Nucl. Instrum. Meth.* **A499** (2003) 469–479.

[9] P. M. Nadolsky and C. P. Yuan *Nucl. Phys.* **B666** (2003) 31–55.

[10] K. Melnikov and F. Petriello *Phys. Rev.* **D74** (2006) 114017.

[11] A. D. Martin, R. G. Roberts, W. J. Stirling, and R. S. Thorne *Eur. Phys. J.* **C28** (2003) 455–473.

[12] A. D. Martin, W. J. Stirling, R. S. Thorne, and G. Watt *Eur. Phys. J.* **C63** (2009) 189–285.